W and Z physics with the ATLAS detector

N. Makovec

W and Z physics with the ATLAS detector

N. Makovec
Laboratoire de l'Accélérateur Linéaire d'Orsay

We present measurements involving W and Z boson production in pp collisions at $\sqrt{s}$=7 TeV with an integrated luminosity of $\sim$35 pb^{-1} recorded by the ATLAS detector at the Large Hadron Collider. Several analysis are presented: Drell-Yan $W \to \ell\nu$ and $Z/\gamma^* \to \ell\ell$ ($\ell = e, \mu$) production cross sections, muon charge asymmetry from W boson decays, production of jets in association with a Z/γ^*boson in the final state and diboson production ($W\gamma$,$Z\gamma$,W^+W^-). The measurements are compared to perturbative QCD predictions with various parton distribution functions.

1 Introduction

The leptonic decays of W and Z bosons provide a very clean experimental signature with which to measure their production cross sections and test the predictions from perturbative Quantum ChromoDynamics (pQCD) at the Large Hadron Collider (LHC) and the accuracy of Parton Distribution Functions (PDF) which parameterize the parton's momentum distribution in the proton. Measurements of such processes, in particular in association with jets, are also important to control backgrounds to other Standard Model measurements like the top cross-section measurement [1] or to searches for physics beyond the Standard Model like the search for squark and gluino production [2]. Here we report measurements involving W and Z boson production in pp collisions at $\sqrt{s}$=7 TeV with an integrated luminosity of $\sim$35 pb^{-1}.

2 Measurement of the total $W^{\pm}$ and Z/γ^* cross sections and muon charge asymmetry

The total W and Z cross section is measured using the following formula:

$$\sigma_{tot} = \sigma_{W/Z} \times BR(W/Z \to \ell\nu/\ell\ell) = \frac{N - B}{A_{W/Z}.C_{W/Z}.L_{int}} \,. \tag{1}$$

Here N is the number of candidate events measured in data, B the number of background events, determined using data and simulation and L_{int} the integrated luminosity corresponding to the run selections and trigger employed. $BR(W/Z \to \ell\nu/\ell\ell)$ stands for branching ratio. The correction by the efficiency factor $C_{W/Z}$, measured partly with data, determines the integrated cross sections σ_{fid} within the fiducial regions of the measurement, while the acceptance factor $A_{W/Z}$, estimated from Monte-Carlo, is introduced to extrapolate the measurement of σ_{fid} to the full kinematic region which determines the total cross section, σ_{tot}. The details of the analysis can be found in Reference [3]. As shown in Figure 1, the measured $W^{\pm}$ and Z/γ^* cross sections

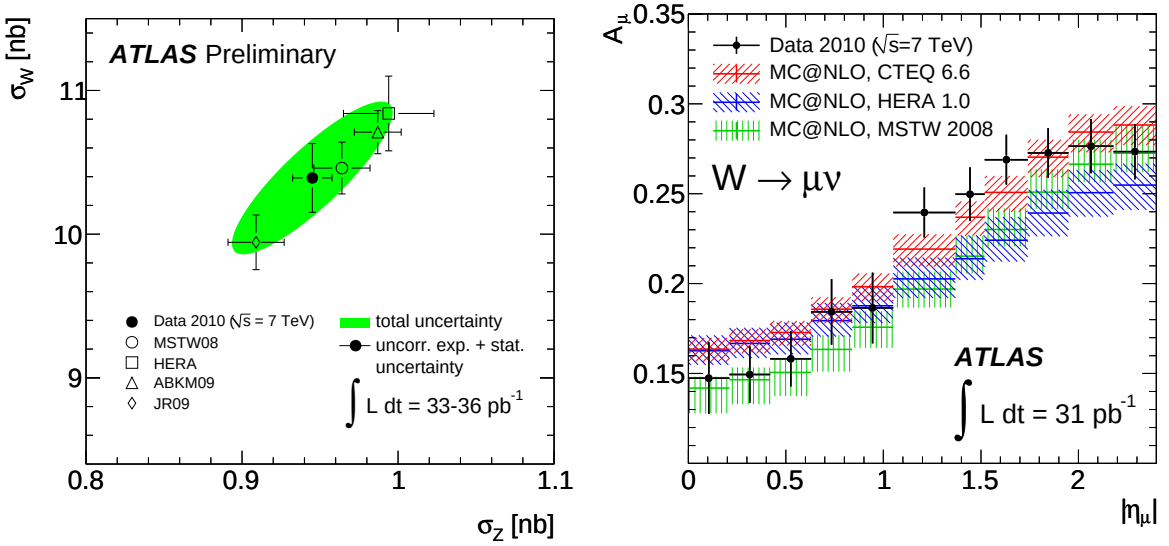

Figure 1: To the left, measured and predicted cross sections times leptonic branching ratios: $(\sigma_{W^+} + \sigma_{W^-})$ vs σ_{Z/γ^*}. The projections of the ellipse to the axes correspond to one standard deviation uncertainty of the cross sections. To the right, the muon charge asymmetry from W-boson decays in bins of absolute pseudorapidity. The data points (shown with error bars including the statistical and systematic uncertainties) are compared to MC@NLO predictions with different PDF sets.

are found to be described by Next-to-Next-to-Leading Order (NNLO) QCD calculations based on a number of different PDF sets.

In pp collisions the overall production rate of W^+ bosons is significantly larger than the corresponding W^- rate, since the proton contains two u and one d valence quarks. The measurement of the lepton charge asymmetry:

$$A_l = \frac{d\sigma_{\mathrm{Wl^+}}/d\eta_l - d\sigma_{\mathrm{Wl^-}}/d\eta_l}{d\sigma_{\mathrm{Wl^+}}/d\eta_l + d\sigma_{\mathrm{Wl^-}}/d\eta_l}\,, \tag{2}$$

can contribute significantly to the understanding of PDFs in the parton momentum fraction range $10^{-3} < x < 10^{-1}$. Systematic effects on the W-production cross-section measurements are typically the same for positive and negative muons, mostly canceling in the asymmetry. Measurements in the muon channel are presented in Figure 1 together with predictions obtained with MC@NLO [4] and different PDF sets. More details can be found in Reference [5]. The data are roughly compatible with all the predictions with different PDF sets, though some are slightly preferred to others. The data presented here are expected to contribute to the determination of the next generation of PDF sets, helping to reduce their uncertainties, particularly the shapes of the valence quark distributions in the low-x region.

3 Measurement of the production cross section for Z/γ^* in association with jets

Production of jets of particles in association with a Z/γ^* boson in the final state was measured. Jets are defined using the anti$-\mathrm{k_T}$ algorithm with $R = 0.4$ and the measurements are performed for jets in the region $p_T^{jet} > 30$ GeV and $|\eta^{\mathrm{jet}}| < 2.8$. The full analysis is described in Reference [6] and the measured cross section as a function of the inclusive jet multiplicity for the electron channel and as a function of p_T^{jet} for the muon channel are presented in Figure 2. The measured cross sections are well described by Next-to-Leading Order (NLO) pQCD predictions obtained by MCFM [7] and including non-perturbative corrections, as well as by the predictions from LO matrix elements supplemented by parton showers, as implemented in the ALPGEN [8] and

SHERPA [9] MC generators but not by PYTHIA [10] which underestimates the measured cross sections.

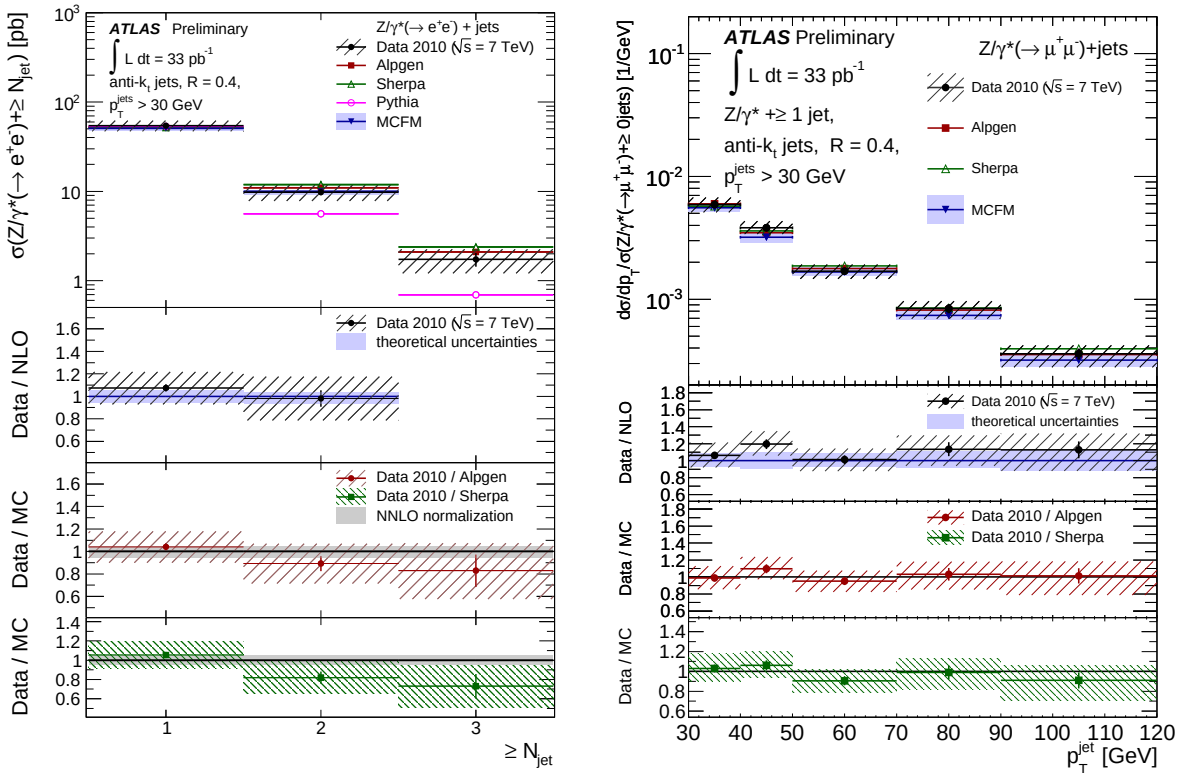

Figure 2: To the left (resp. right), measured cross section (black dots) in $Z/\gamma^*(\rightarrow e^+e^-)$+jets (resp. $Z/\gamma^*(\rightarrow \mu^+\mu^-)$+jets) production as a function of the inclusive jet multiplicity (resp. p_T^{jet}), for events with at least one jet with $p_T^{jet} > 30$ GeV and $|\eta^{\rm jet}| < 2.8$ in the final state. The error bars indicate the statistical uncertainty and the dashed areas the statistical and systematic uncertainties added in quadrature. The measurements are compared to NLO pQCD predictions from MCFM (only available up to 2 jets), as well as the predictions from ALPGEN, SHERPA, and PYTHIA. The shadowed areas around the ALPGEN and SHERPA predictions denote a 5% uncertainty on the absolute normalization.

4 Measurement of diboson production ($W\gamma$,$Z\gamma$,W^+W^-)

ATLAS has also performed the measurement of diboson production of high energy photons in association with either a W or Z boson. Such measurements allow to test pQCD. Moreover, the $W\gamma$ process includes a diagram sensitive to Triple Gauge boson Coupling (TGC) of the electroweak sector. Events with W and Z bosons decaying into high-p_T electrons and muons are required in addition to have a photon with $E_T > 15$ GeV located outside a cone of radius 0.7 in η - ϕ space centered on the lepton(s) from the boson decay. To further reduce the background due to photons from π^0 and η decays, an isolation requirement of $E_T^{iso} < 5$ GeV is applied. E_T^{iso} is the total transverse energy recorded in the calorimeter in a cone of radius 0.4 around the photon direction (excluding a small window which contains the photon energy). E_T^{iso} is corrected for the leakage of the photon energy into the isolation cone and the contributions from the underlying and pile-up activities in the event. A total of 95 (97) $pp \rightarrow e\nu\gamma + \mathrm{X}$ ($pp \rightarrow \mu\nu\gamma + \mathrm{X}$) and 25 (23) $pp \rightarrow e^+e^-\gamma + \mathrm{X}$ ($pp \rightarrow \mu^+\mu^-\gamma + \mathrm{X}$) event candidates are selected [11]. The measured production cross sections, together with the kinematic distributions of the leptons and photons in data signal candidate events, are found to agree with the $O(\alpha\alpha_s)$ Standard Model predictions (see Table 1).

	Experimental measurement $\sigma^{total}[pb]$(measured)	SM model prediction $\sigma^{total}[pb]$(predicted)
$pp \to e\nu\gamma$	$73.9 \pm 10.5(stat) \pm 14.6(syst) \pm 8.1(lumi)$	69.0 ± 4.6(syst)
$pp \to \mu\nu\gamma$	$58.6 \pm 8.2(stat) \pm 11.3(syst) \pm 6.4(lumi)$	69.0 ± 4.6(syst)
$pp \to e^+e^-\gamma$	$16.4 \pm 4.5(stat) \pm 4.3(syst) \pm 1.8(lumi)$	13.8 ± 0.9(syst)
$pp \to \mu^+\mu^-\gamma$	$10.6 \pm 2.6(stat) \pm 2.5(syst) \pm 1.2(lumi)$	13.8 ± 0.9(syst)

Table 1: Total cross sections of the $pp \to l\nu\gamma + X$ and $pp \to ll\gamma + X$ process at $\sqrt{s} = 7\ TeV$. Both, experimental measurement and SM model NLO prediction are given. The total cross sections are measured with $p_T(\gamma) > 10\ GeV$, $\Delta R(l,\gamma) > 0.5$ and $\epsilon_h^p < 0.5$ where ϵ_h^p is defined at particle level as the ratio between sum of the energies carried by final state particles in the cone $\Delta R < 0.4$ around the photon and the energy carried by the photon.

The WW production cross section in pp collisions was also measured using three leptonic decay channels: electron-electron, muon-muon and muon-electron channels. Such processes are also sensitive to TGC as predicted by the Standard Model. The decay products from both top-pair ($t\bar{t} \to WbWb$) and single top ($tW \to WbW$) processes contain also WW in the final states. The top events are characterized by hadronic jet activity in the final state. Using a jet-veto cut the majority of the top background can be removed from the WW event selection. A total of eight candidates are selected with an estimated background of 1.7 ± 0.6 events. The probability for the estimated background to fluctuate up to at least the observed eight events is $1.4{\times}10^{-3}$, corresponding to a signal significance of 3.0 standard deviations. The measured cross section is 40^{+20}_{-16}(stat)$\pm$7(syst) pb, consistent with the SM NLO prediction of 46 ± 3 pb.

5 Summary

First measurements involving W and Z boson production in pp collisions at $\sqrt{s}$=7 TeV with an integrated luminosity of $\sim$35 pb^{-1} recorded by the ATLAS detector at the Large Hadron Collider were presented. Theoretical predictions are in good agreement with all measurements within statistical and systematic uncertainties. The increase of integrated luminosity with 2011 data will permit more stringent test of perturbative QCD and tighter constraints on parton distribution functions.

References

1. G. Aad *et al.* [ATLAS Collaboration], Eur. Phys. J. C **71** (2011) 1577.
2. G. Aad *et al.* [ATLAS Collaboration], Phys. Lett. B **701** (2011) 186.
3. ATLAS Collaboration, ATLAS-CONF-2011-041, `https://atlas.web.cern.ch/Atlas/GROUPS/PHYSICS/CONFNOTES/ATLAS-CONF-2011-041`.
4. S. Frixione and B. R. Webber, JHEP **0206** (2002) 029.
5. G. Aad *et al.* [ATLAS Collaboration], Phys. Lett. B **701** (2011) 31.
6. ATLAS Collaboration, ATLAS-CONF-2011-042, `https://atlas.web.cern.ch/Atlas/GROUPS/PHYSICS/CONFNOTES/ATLAS-CONF-2011-042`.
7. J. M. Campbell and R. K. Ellis. Phys. Rev. D **65** (2002) 113007.
8. M. L. Mangano *et al.* JHEP **0307** (2003) 001.
9. T. Gleisberg *et al.* JHEP **0902** (2009) 007.
10. T. Sjostrand, S. Mrenna and P. Z. Skands, JHEP **0605** (2006) 026.
11. ATLAS Collaboration, ATLAS-CONF-2011-013, `https://atlas.web.cern.ch/Atlas/GROUPS/PHYSICS/CONFNOTES/ATLAS-CONF-2011-013`.
12. ATLAS Collaboration, ATLAS-CONF-2011-015, `https://atlas.web.cern.ch/Atlas/GROUPS/PHYSICS/CONFNOTES/ATLAS-CONF-2011-041`.